



Universiteit
Leiden
The Netherlands

Quantification of GPCR internalization by single-molecule microscopy in living cells

Serge, A.; Keijzer, S. de; Hemert, F. van; Hickman, M.; Hereld, D.; Spaink, H.P.; ... ; Snaar, B.E.

Citation

Serge, A., Keijzer, S. de, Hemert, F. van, Hickman, M., Hereld, D., Spaink, H. P., ... Snaar, B. E. (2011). Quantification of GPCR internalization by single-molecule microscopy in living cells. *Integrative Biology*, 3(6), 675-683. doi:10.1039/c0ib00121j

Version: Publisher's Version

License: [Licensed under Article 25fa Copyright Act/Law \(Amendment Taverne\)](#)

Downloaded from: <https://hdl.handle.net/1887/3736453>

Note: To cite this publication please use the final published version (if applicable).

Cite this: *Integr. Biol.*, 2011, **3**, 675–683

www.rsc.org/ibiology

PAPER

Quantification of GPCR internalization by single-molecule microscopy in living cells†

Arnauld Sergé,^{‡a} Sandra de Keijzer,^{‡ab} Freek Van Hemert,^{ab} Mark R. Hickman,^c Dale Hereld,^d Herman P. Spalink,^b Thomas Schmidt^a and B. Ewa Snaar-Jagalska^{*b}

Received 18th October 2010, Accepted 23rd March 2011

DOI: 10.1039/c0ib00121j

Receptor internalization upon ligand stimulation is a key component of a cell's response and allows a cell to correctly sense its environment. Novel fluorescent methods have enabled the direct visualization of the agonist-stimulated G-protein-coupled receptors (GPCR) trafficking in living cells. However, it is difficult to observe internalization of GPCRs *in vivo* due to intrinsic autofluorescence and cytosolic signals of fluorescently labeled GPCRs. This study uses the superior positional accuracy of single-molecule fluorescence microscopy to visualize in real time the internalization of *Dictyostelium discoideum* cAMP receptors, cAR1, genetically encoded with eYFP. This technique made it possible to follow the number of receptors in time revealing that the fraction of cytosolic receptors increases after persistent agonist stimulation and that the majority of the receptors were degraded after internalization. The observed internalization process was phosphorylation dependent, as shown with the use of a phosphorylation deficient cAR1 mutant, cm1234-eYFP, or stimulation with an antagonist, Rp-cAMPS that does not induce receptor phosphorylation. Furthermore, experiments done in mound-stage cells suggest that intrinsic, phosphorylation-induced internalization of cAR1 is necessary for *Dictyostelium* wild type cells to progress properly through multicellular development. To our knowledge, this observation illustrates for the first time phosphorylation-dependent internalization of single cAR1 molecules in living cells and its involvement in multicellular development. This very sensitive imaging of receptor internalization can be a useful and universal approach for pharmacological characterization of GPCRs in other cell types.

^a From *Physics of Life Processes*, Leiden Institute of Physics, Leiden University, P.O. Box 9504, Leiden, The Netherlands

^b IBL Molecular Cell Biology, Leiden University, Gorlaeus Laboratory, Einsteinweg 55, 2333 CC Leiden, P.O. Box 9504, Leiden, The Netherlands.
E-mail: B.E.Snaar-Jagalska@biology.leidenuniv.nl;
Fax: 31-71-5274357; Tel: 31-71-5274980

^c Division of Experimental Therapeutics, Walter Reed Army Institute of Research, Silver Spring, MD 20910, USA

^d Division of Metabolism and Health Effects, National Institute on Alcohol Abuse and Alcoholism, NIH, Rockville, MD 20852, USA

† Electronic supplementary information (ESI) available. See DOI: 10.1039/c0ib00121j

‡ Authors contributed equally to this work.

Introduction

In the majority of signaling events initiated by extra-cellular ligands, such as hormones, neurotransmitters and growth factors, the binding of these signaling molecules to seven *trans*-membrane G-protein-coupled receptors (GPCRs) results in the activation of G-proteins localized at the inner face of the plasma membrane.^{1–3} In addition, agonist activation of a GPCR also results in (i) receptor internalization, (ii) feedback regulation of G-protein coupling and (iii) signaling through G-protein independent pathways.⁴ GPCR activity is the result of the coordinated

Insight, innovation, integration

G-Protein Coupled Receptors are the most important drug targets and considering GPCRs need to be accessible to the drug, knowledge on GPCR internalization will minimize effective drug concentration in therapies. However, it is difficult to observe internalization of GPCRs *in vivo* due to intrinsic fluorescence and cytosolic signals of fluorescently labeled GPCRs. To overcome this problem, this study used

the superior resolution of single-molecule fluorescence microscopy to visualize the debated internalization of *Dictyostelium discoideum* cAMP receptors. The positional accuracy obtained by our method allowed for the quantification of internalized cAR1s upon stimulation in live cells for the first time and we showed that this is phosphorylation dependent and important for development.

balance between these inter-related processes which govern receptor signaling, desensitization and resensitization. It has been suggested that the function of ligand-induced internalization of GPCRs in the desensitization and resensitization mechanisms is dependent on the type of receptor trafficking which is different for different subtypes of GPCRs.⁴ Therefore to understand the function of GPCR internalization it is necessary to unravel the mechanism of internalization in terms of quantity, how many receptors are internalized, of timescale, what is the onset and duration of internalization, and of process, by which endocytic pathway does internalization occur. Upon internalization receptors can be either recycled back to the plasma membrane (resensitization) or degraded (“down-regulated”) in lysosomes. Importantly, the internalized receptors can also be involved in intracellular signaling (*e.g.*, MAPK and transcriptional regulation)⁵ Here, these processes were investigated by single-molecule microscopy which allowed us to follow GPCR internalization one-by-one with much higher spatial-temporal precision compared to conventional fluorescent methods. As a model we chose the cyclic adenosine mono-phosphate receptor in the well studied model organism *Dictyostelium discoideum*.

It has been long established that the eukaryotic social amoeba *D. discoideum* senses chemoattractants (like cAMP) by the same signal transduction mechanisms as many hormones, neurotransmitters, odorants in mammals.^{6,7} Cloning and deletion of the four 7-TM cAMP receptors (cAR1-cAR4) showed that they are essential for chemotaxis and for the developmental cycle of *D. discoideum*.⁸⁻¹¹ Development of *Dictyostelium* is initiated by nutrient depletion and during the first few hours of starvation, subsets of cells periodically secrete a pulse of the chemoattractant cAMP. The secreted cAMP signal is perceived by cells *via* cAMP receptors (cARs), which, in turn, trigger the synthesis and secretion of additional cAMP to relay the signal, creating an outwardly radiating cAMP gradient.^{12,13} Simultaneously, cells within the cAMP gradient become polarized, oriented, and chemotactic towards the direction of the highest concentration of cAMP and move inward.¹² Cells also quickly adapt to the cAMP signal,¹⁴ but as extracellular cAMP is degraded by secreted phosphodiesterase, cells reacquire sensitivity for the next cAMP pulse emanating from the signaling center.¹⁵ Adaptation/deadaptation not only provides a robust directional chemoattractant gradient but also ensures that cells within a signaling territory are laterally inhibited from establishing secondary centers that would disrupt wave propagation and aggregation.¹⁶ At ~ 10 h, 10^5 aggregating cells form mounds at these signaling centers, which continue to develop into the terminally differentiated mature fruiting bodies within another 15 h cAMP levels are considered to increase to micromolar concentration during development due to reduction of intracellular space in the compact mound structure leading to expression of genes required for completion of the developmental program.^{17,18}

The function of cAR1 internalization in the developmental program of *D. discoideum* is poorly understood and in fact cAR1 internalization itself is highly debated. Previous immunofluorescence studies have shown that ligand occupancy of the primary cAMP receptor, cAR1 can lead to its clustering or internalization.¹⁹ In contrast, more recent evidence indicated

that cAR1 remained uniformly distributed on the plasma membrane even after prolonged cAMP stimulation.²⁰ However, data obtained from these types of fluorescence microscopy studies are difficult to interpret because of cell-specific autofluorescence and high fluorescence signal from the labeled receptor, since the fluorescent receptor was expressed at the endogenous level.

GPCR phosphorylation is known to regulate processes like receptor internalization and desensitization.^{21,22} As in other systems, the cytosolic C-terminal tail of cAR1 can be phosphorylated and cells expressing a cAR1 receptor lacking the C-terminal tail phosphorylation sites revealed that cAR1 phosphorylation is associated with a reduction in the receptor's affinity.²³⁻²⁶ However, ligand-induced phosphorylation seemed to have little impact on the overall adaptation of cAR1-mediated pathways.^{23,24} Cells expressing the phosphorylation deficient mutant did exhibit delayed asynchronous development and many aggregates arrest at the mound stage. The prestalk-specific *ecmA* gene expression was reduced and this may account for the morphological defects since prestalk cell differentiation is needed for tip formation.²⁷⁻²⁹

In this article, we investigate, in real time, the internalization of cAR1 on external stimulation by cAMP *in vivo* by single-molecule microscopy. The high spatio-temporal precision of this technique allows for the identification of single cAR1-eYFP molecules both in the plasma membrane and cytosol and dynamic changes can be followed. Our results prove that cAR1 receptors are internalized upon persistent stimulation with cAMP on a timescale of $t_{1/2} = 5$ min followed by degradation $t_{deg} = 13$ min and that this process requires receptor phosphorylation. Furthermore, cAR1 receptors are primarily localized in the cytosol in cells isolated from the mound stage in contrast to the phosphorylation deficient mutant receptor which remains on the plasma membrane in cells from the mound stage. This lack of intrinsic-phosphorylation dependent internalization could account for the documented developmental arrest in the mutant and suggest that phosphorylation-dependent cAR1 internalization is a component of the cell physiological response during development.

Results and discussion

Detection of single-molecule GPCRs in living cell

Investigation of receptor internalization at the single molecule level in live cells was performed by focusing into the median plane of *D. discoideum car1⁻* cells transformed with cAR1-eYFP (Fig. 1). This protein is functionally indistinguishable from wild-type cAR1 and allowed us to visualize receptors during stimulus presentation in live cells.³⁰ Single-molecule microscopy (SMM) was used to obtain high spatial (~ 40 nm) and temporal (~ 5 ms) precision information on cAR1 receptors.³¹ In order to reach a density of fluorescent receptors at which individual molecules could be observed ($< 1 \mu\text{m}^{-1}$), cells were photobleached prior to imaging.³⁰ It should be noted that the unbleached population of receptors is a fully representative subpopulation of all receptors since photobleaching is a random process. The remaining, well-separated fluorescent signals were localized with high accuracy by describing the observed

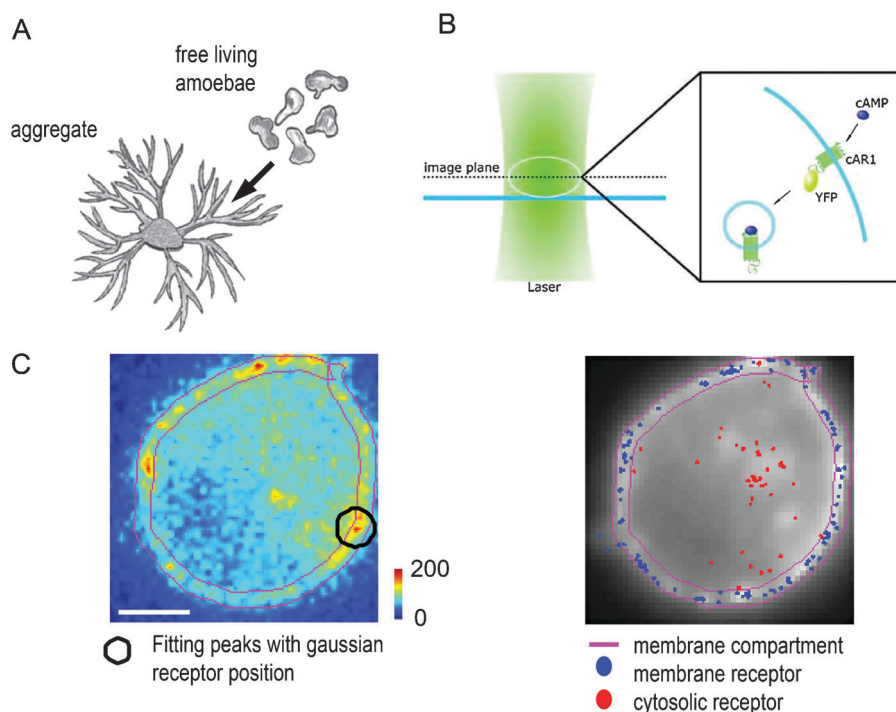


Fig. 1 Detection of single cAR1-eYFP molecules. (A) *D. discoideum* cells live as single cells in the soil. Upon starvation they secrete cAMP and chemotact towards each other to form a multi-cellular organism, which undergoes multiple developmental changes. (B) *car1*⁻ cells transformed with cAR1-eYFP were stimulated with cAMP. The receptor was imaged by fluorescence microscopy. (C) The left image presents the middle plane of a typical unstimulated *car1*⁻ *D. discoideum* cell transformed with cAR1-eYFP with the position of the membrane compartment (magenta). The right image is a superposition of the mean image of a stack and that of all single-molecule positions (blue-membrane, and red-cytosol). The membrane compartment was defined by a width of 600 nm (magenta). This value accounts both for membrane fluctuations during recording and the optic resolution. This allows an estimation of the percentage of receptors remaining at, or near, the membrane. The scale bar is 5 micron long.

signals with a Gaussian spread-function and calculating the centre. This analysis allowed for the localization of an observed signal with a positional accuracy of 40 nm. The obtained signals were further analyzed to identify them as individual emitting eYFP molecules³² from the autofluorescence. Fluorescence signals from individual molecules exhibited similar intensity profiles as single eYFPs immobilised in a gel³³ and single-step photobleaching typical of single molecules (Fig. S1†).³⁰

The cell was divided in a plasma membrane compartment and a residual cytosolic compartment including the endocytic vesicles in which internalized receptors are expected to be found. By observation in the median plane it was possible to simultaneously image receptors located in the plasma membrane and those located in the cytosol. The position of the plasma membrane was determined from the mean of the whole image stack (Fig. 1C). For analysis, a plasma membrane compartment with a width of 660 nm (3 pixels) was defined which takes into account both the optical resolution of the microscope ($0.61 \cdot \lambda / \text{NA} = 224 \text{ nm}$) and any fluctuations of the membrane position during the length of the recording (5–25 s), in agreement with distance distributions obtained on control data. It should be noted that this size is much larger than the actual width of the plasma membrane (5 nm) and as a result, the fraction of receptors at the membrane reported in the current study was in fact over-estimated by including receptors located close to the plasma membrane. However, the error introduced

by this definition was assumed to be small since receptor concentration was much higher at the plasma membrane compared to that in the cytosol (see Fig. 2A, 3A and B). Indeed, calculations with different membrane thicknesses (2–4 pixels) showed no significant changes in receptor fractions localized in the membrane and cytosol resp. (Fig. S2A†). In addition the estimated plasma membrane compartments were comparable with concanavalin A-Alexa 647 staining of the plasma membrane (Fig. S2B†).

cAR1 is internalization upon cAMP stimulation

The localization and the behavior of the receptors were followed on single cells by recording image stacks at different time points before and upon continuous stimulation with 10 μM cAMP. Real time measures of single receptors within a live amoeba were directly illustrated in the movie (ESI movie M1†). Analysis of the image stacks localized the receptors in either the plasma membrane or the cytosolic compartment. The fraction of receptors found at the plasma membrane decreased with 55% after 30 min of cAMP stimulation as compared to before stimulation (Fig. 2A). We blocked *de novo* protein synthesis by supplementing the medium with 90 μM cycloheximide 1 h before and during the experiment, therefore we can attribute the loss of plasma membrane localized receptors to internalization. These measurements were taken by focusing in the middle of the cell and therefore we calculated how this

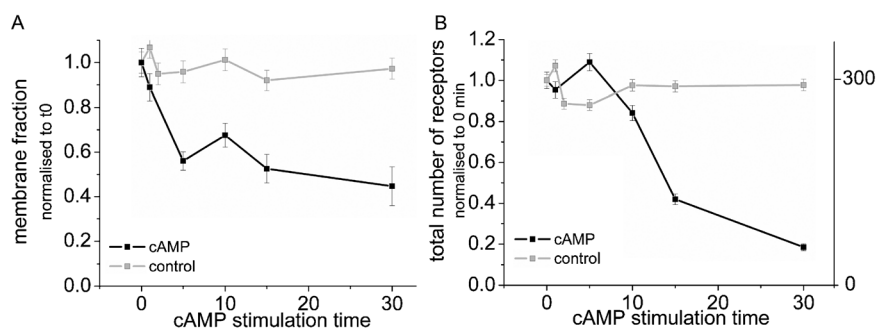


Fig. 2 Internalization of cAR1-eYFP followed on a single cell. Internalization before and after stimulation (10 μ M cAMP) was followed on a single cell, by recording stacks of 100 images at the indicated time points. (A) Graph of the fraction of receptors remaining at the membrane *versus* time after stimulation normalized to t0. The fraction is decreased with time of stimulation. This shows that receptors were internalized after stimulation. (B) Graph of the total number of receptors *versus* time, depicting receptor degradation after stimulation, plotted in relative (left) or total (right) number. In this experiment, *de novo* protein synthesis was suppressed by 90 μ M cycloheximide. Error bars correspond to *s.e.* These results are representative examples of 47 cells in 5 experiments.

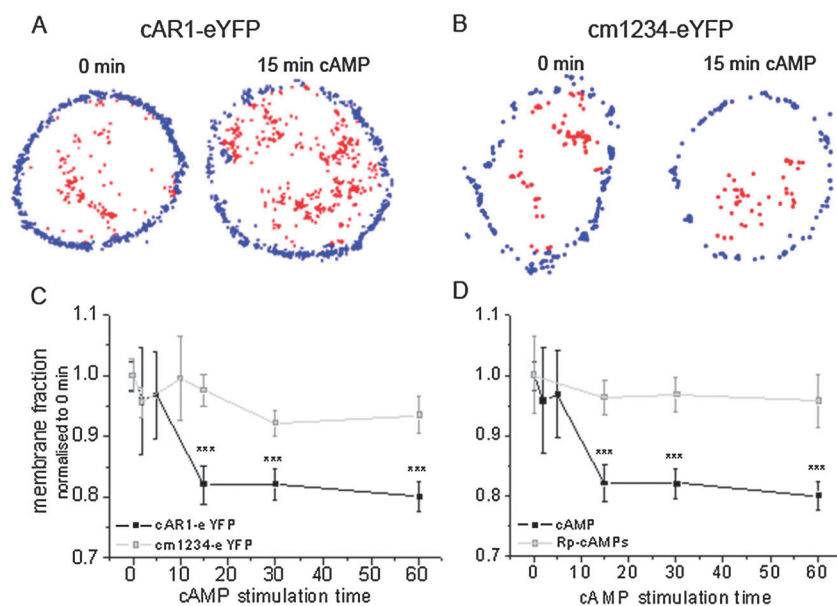


Fig. 3 Phosphorylation does affect receptor localization at the membrane. (A), (B) Typical cells measured at 10 $^{\circ}$ C, expressing either cAR1-eYFP (A) or cm1234-eYFP (B) before or after 15 min stimulation with 10 μ M cAMP. The fraction of molecules in the cytoplasm is increased after 15 min of stimulation for cAR1-eYFP, but not for the phosphorylation deficient mutant cm1234-eYFP. (C) Graph of the fraction remaining at the membrane *versus* time after stimulation, normalized at 0 min for comparison. This fraction significantly decreased in time for cAR1-eYFP, but not for cm1234-eYFP. (D) The fraction remaining at the membrane significantly decreased in time for cAR1-eYFP when stimulated by cAMP, but not when stimulated by the antagonist Rp-cAMPS, which binds to the receptors without inducing their phosphorylation. Error bars correspond to *s.e.m.*

55% decrease in membrane receptor fraction translates to the whole cell (see Materials and methods). Assuming that receptor localization is not polarized but homogeneous over the whole cell (as reported before),^{19,20} the ratio of receptors located at the membrane in the median plane is proportional to the total ratio for the whole cell. The correction factor is 3/2 (see Materials and methods) and the measured 55% decrease relates to an 83% decrease in plasma membrane localized receptors for the whole cell. The membrane receptor fraction remained almost constant over time for an unstimulated control-cell, indicating that the cAMP-induced reduction is not a photo-bleaching artifact during the measurement, but is specific to an active agonist induced mechanism (Fig. 2A). We observed that before stimulation, 72% of the total receptors counted were localized in the

plasma membrane. Since we suppressed biosynthesis of receptors, this suggests that there was a constitutive internalization of the receptors by the cells, and that this internalization was increased on persistent stimulation.

The trafficking of receptors upon internalization was further investigated, concerning recycling and/or degradation of the receptors. The total number of receptors after photobleaching was computed at each stimulation time point. As seen in Fig. 2B, this total number was decreased after stimulation, from $N = 305$ to $N = 60$, showing that 80% of the receptors were degraded after 30 min of cAMP stimulation. The typical time of internalization $t_{1/2} = 5$ min (Fig. 2A), precedes that of degradation $t_{deg} = 13$ min (Fig. 2B), as was expected for a sequential process. Little variation was observed for the unstimulated control-cells,

again showing that photobleaching is not affecting the results (Fig. 2B).

Further characterization revealed that the dynamics of the majority (70%) of single receptors in the cytosolic compartment was not significantly different from the dynamics of plasma membrane localized receptors. We concluded from this analysis that the majority of molecules observed in the cytosolic compartment were not freely diffusing in the cytosol and we assumed the receptors being internalized *via* vesicular transport (Fig. S3†). The small fraction (30%) of fast receptors in the cytosol could reflect a population of freely diffusing cAR1-eYFP or eYFP removed from the cAR1 receptor.

In relation to earlier studies by confocal microscopy in which the total fluorescence of the membrane compartment was compared to that in the cytosol, the results from our single-molecule approach was less influenced by cellular autofluorescence since only signals identified as individual cAR1-eYFP were taken into account in the analysis. As a result we were able to quantitatively prove that cAR1 internalization occurs upon global cAMP stimulation.

Variation in cell populations

Obtaining sufficient statistics is a time-consuming process when following internalization on one cell for a long period of time; therefore we wanted to change the set-up of the experiments. We stimulated a population of cells with cAMP for a given time (0–60 min), washed the cells in phosphate buffer, and subsequently imaged and analyzed multiple cells in the population. In order to synchronize the period of stimulation for the whole population in one experiment, the cells were maintained at 10 °C to slow down de-phosphorylation kinetics. This temperature was found to be a good compromise between the maintenance of the cell metabolism and the reduction of the de-phosphorylation kinetics. Since it was previously shown that incubation at 4 °C kept the cAMP stimulated receptors in their phosphorylated state for at least two hours upon removal of cAMP,²⁰ the duration of an experiment was limited to 30 min to minimize significant metabolic differences between cells. Fig. 3A depicts two cells showing that in those conditions the fraction of receptors at the plasma membrane is reduced after stimulation. Indeed, analysis revealed that the mean membrane receptor fraction ($N > 30$ cells for each timepoint) is decreased significantly after cAMP stimulation by at least 20%, corresponding to 30% for the whole cell membrane. The small decrease found in comparison with the measurements on single cells reflects a high variation in the population of cells. Notwithstanding, the same dynamics of internalization process was observed with $t_{1/2} = 5$ min. This experimental set-up, which did not require observing individual cells over an extended period of time, significantly reduced the experimental complexity in subsequent mutant studies.

Phosphorylation requirement for internalization

We wanted to study whether cAR1 internalization is a phosphorylation-dependant process as predicted and used a phosphorylation deficient receptor mutant genetically encoded with eYFP, cm1234-eYFP. This mutant has all putative phosphorylation residues (18 serines) from the cytosolic C-terminus

substituted, completely abolishing the cAMP-dependent electrophoretic mobility shift of purified receptors, which is associated with cAR1 phosphorylation³⁴ (Fig. S4†). In contrast to cAR1-eYFP (Fig. 3A) the phosphorylation deficient receptor, cm1234-eYFP, was not internalized on stimulation (Fig. 3B). The mean fraction of receptors staying at the membrane was decreased significantly by at least 20% for cAR1-eYFP upon stimulation, while this fraction remained almost constant for cm1234-eYFP (Fig. 3C). It should be noted that expression of cAR1-eYFP and cm1234-YFP in wild type strains (data not shown) led to identical results, indicating that the observed results was not caused by additional defects in the *car1*⁻ cells. Similarly to the results obtained with cm1234-eYFP, the antagonist Rp-cAMP, which binds to the cAR1-eYFP without inducing its phosphorylation^{35,36} did not cause a redistribution of cAR1-eYFP between membrane-bound and cytosolic fraction (Fig. 3D). These data mutually showed that cAMP induced cAR1 internalization occurs in a phosphorylation-dependent manner.

cAR1 remains phosphorylated in the cytosolic compartment

The expression of membrane and cytosolic fractions of receptors upon cAMP stimulation was detected with western blot (Fig. 4). The method we used allowed for the separation of the plasma membrane from cytosolic compartmental membranes.³⁷ In untreated cells (0 min) the eYFP antibody detected a fusion protein of the expected size (70 kDa) mainly in the membrane fraction. Fig. 4 further shows an increase in the cytosolic fraction and a decrease in membrane bound fraction after agonist treatment. In addition, cAMP stimulation induced a shift of the receptor fusion protein to a form with a lower electrophoretic mobility in both membrane and cytosolic fraction. This shift was also observed for wild-type cAR1 and is known to be due to phosphorylation of cAR1 on either Ser-303 or 304.^{23,34} The cytosolic fraction, reflecting the internalized receptors, remained stably phosphorylated after global stimulation, indicating that the phosphorylation state of cAR1-eYFP fusion protein was unchanged during cAMP induced internalization. The fact that only ~50% of the cAR1-eYFP was upshifted after 15 min incubation with 10 μM cAMP, a condition that resulted in over 95% upshift of wild-type cAR1,²⁵ suggests that the C-terminal eYFP moiety either decreases the kinetics of phosphorylation (or increases dephosphorylation), or renders a fraction of the receptor inaccessible to the kinase responsible

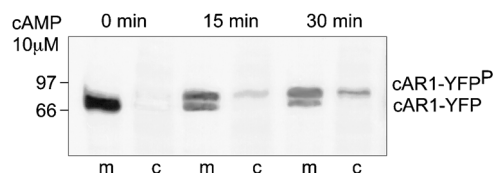


Fig. 4 Gel mobility shift assay. Western-blots of membrane (m) and cytosolic (c) fractions of cAR1-eYFP, before and 15 or 30 min after stimulation with cAMP. The eYFP antibody detected a fusion protein of the expected size (70 kDa) mainly in the membrane fraction in treated cells (0 min). cAMP stimulation increased the cytosolic fraction and decreased the membrane bound fraction and in addition induced a shift of the receptor fusion protein to a form with a lower electrophoretic mobility in both membrane and cytosolic fraction.

for phosphorylation. Post-lysis dephosphorylation could also explain this observation.

Internalization is part of dictyostelium development program

Previously, it has been shown that cells expressing the mutant receptor cm1234 in a *car1/3-null* background exhibit a pattern of developmental defects that indicate a role for the C-terminal tail, and possibly its phosphorylation, in morphogenesis and the expression of cell-type-specific genes. The observed defects are manifested primarily after aggregation, at the transition between the mound and the formation of the culminate.²⁹ The cells displayed delayed asynchronous development and many aggregates arrested at the mound stage. Besides these earlier published morphological phenotypic defects we also observed small aggregates during development (data not shown). To shed more light on the mechanism underlying these observed defects, we looked at the localization of cAR1-eYFP in cells from the mound stage and compared this with the localization of cm1234-eYFP in cells at the mound stage. We found that most of the signals coming from cAR1-eYFP were localized in the cytosol (Fig. 5A). Data analysis revealed that 75% of cAR1-eYFP receptors localized in the cytosol in cells from the mound stage, while only 9% of cAR1-eYFP localized in the cytosol in aggregation competent cells. In contrast, cm1234-eYFP receptors were mainly localized at the plasma membrane in cells from the mound stage, not significantly different from the situation in aggregation competent cells (Fig. 5B). In addition cm1234 expression was prolonged up to 33 h in contrast to wildtype cAR1 which can't be detected after the mound stage (10–16 h)³⁸ of development (Fig. S4†). These data suggest that the intrinsic-phosphorylation dependent internalization

of cAR1 is part of the developmental program and if abolished affects the progression through the developmental cycle.

Discussion

This study used single-molecule imaging techniques, with superior lateral accuracy as compared to regular fluorescence microscopy, to successfully monitor internalization of the G-protein coupled receptor, cAR1, in live *Dictyostelium discoideum* cells. Using single-molecule fluorescence microscopy we have shown that the cAR1-eYFP was partly internalized with $t_{1/2} = 5$ min and degraded with $t_{deg} = 13$ min after persistent cAMP stimulation. As shown by the use of a phosphorylation deficient mutant and an antagonist that does not induce receptor phosphorylation, internalization requires phosphorylation of the receptors to occur.

The literature about internalization of cARs upon stimulation is conflicting. Some earlier studies, based on biochemistry^{39,40} and on immuno-cytochemistry¹⁹ reported internalization, while later studies stated that receptors stayed at the membrane, although dealing with cells in suspension²⁴ or shorter stimulation times.²⁰ Our data now clearly demonstrate cAR1 internalization and the average fraction, as measured with the highly sensitive single-molecule technique on a cell population, is rather low $\sim 30\%$. This could explain why internalization could not be detected by classical methods, since *Dictyostelium discoideum* cells are highly autofluorescent.³²

Upon prolonged stimulation, many GPCRs become phosphorylated and subsequently internalized into endosomes where the receptors can either be recycled back to the plasma membrane, a process called resensitization, or targeted for degradation. The consequent reduction in receptor number as a result of

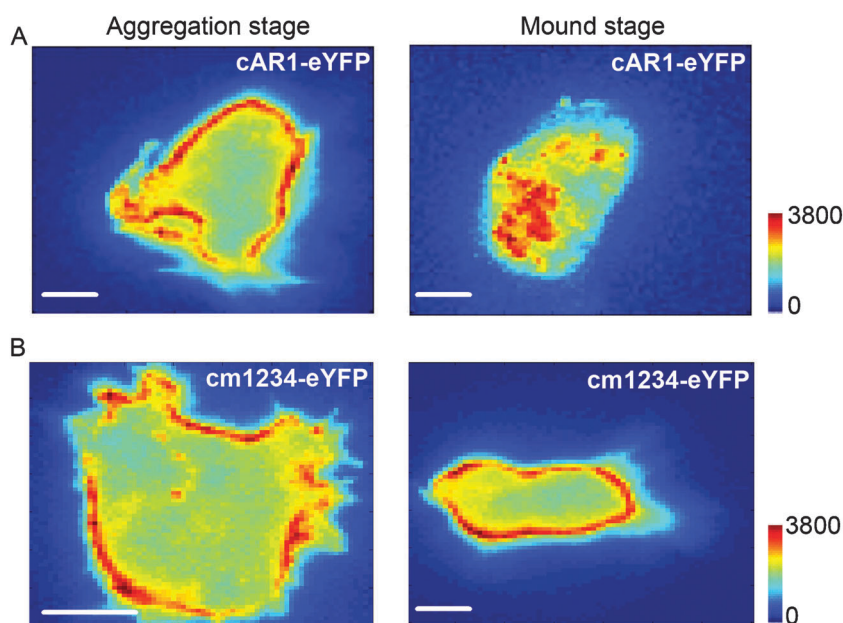


Fig. 5 cAR1 localization is cytosolic in later stages of development. (A) Localization of wild type cAR1-eYFP receptors in aggregation competent cells and in cells which were disaggregated from mounds. Data analysis showed that in aggregation competent cells (14) 9% of receptors were found in the cytosol and in cells from mound (37) 75% of the receptors were found in the cytosol. (B) Localization of cm1234-eYFP receptors in aggregation cells showed that the majority of the receptors localized in the membrane and this is unchanged during development to the mound stage. (All images shown are before photobleaching). The scale bar is 5 microns long.

degradation, known as receptor downregulation, is part of the signal desensitization process.^{41,42} Desensitization of the chemotactic response in *Dictyostelium* is poorly understood but thought of as an integral process of different mechanisms like adaptation, sequestration and down-regulation. Adaptation, the rapid and reversible attenuation of responses to a uniform stimulus of cAMP, is on the order of 20–30 s for many responses and is phosphorylation independent.²⁶ We demonstrated that phosphorylation-dependent internalization of cAR1 upon uniform cAMP stimulation occurs with $t_{1/2} = 5$ min and therefore probably does not account for these fast adaptation responses. However, it was found that uniform chemoattractant stimulation of cells lacking the PIP₃ phosphatase PTEN results in dramatically prolonged PH domain association with the plasma membrane (6–8 min *versus* ~30 s for wild-type).⁴³ Although this observation demonstrated that loss of PTEN leads to a profound loss of adaptation to the chemoattractant signal, the fact that the response eventually subsided after a few minutes implies that there are other mechanisms to downregulate activation⁴⁴ and could indicate that the ligand-induced, receptor phosphorylation dependent internalization we observed is another desensitization mechanism.

Our data established that the major part (80%) of the receptors was degraded after internalization. However, this does not exclude a possible recycling of a sub-fraction of the receptors at the same time, as suggested previously.³⁹ We further demonstrated that cells obtained from the mound stage showed primarily cytosolic cAR1 receptors. One of the key features of *Dictyostelium* development is the presentation of cAMP in the form of a low pulsatile signal during aggregation and at a high, sustained level in the mound.¹⁷ The observed degradation of cAR1 upon cAMP stimulation and the localization cAR1 primarily in the cytosol during mound stage could be part of a desensitization mechanism to cope with the different cAMP levels during development and important for normal progression through the developmental program. Indeed, cells expressing the phosphorylation-deficient mutant receptor cm1234, which were not internalized, primarily localized on the plasma membrane during the mound-stage and showed delayed degradation (Fig. S4†), were shown to have delayed, asynchronous development and many aggregates arrest at the mound stage.²⁹

The different cAMP levels during development can induce different cAMP-receptor dependent signaling pathways, resulting in distinct biological responses.^{45–47} In order to understand the mechanism of activating different signaling pathways, it will be interesting to investigate whether the ligand is internalized together with the receptor, the dynamics of G-proteins during this internalization process (*i.e.* are G-proteins are dissociated from internalized receptors) and if internalized receptors are still able to signal through other pathways, which has been reported for the β -adrenergic receptor and MAPK.⁴⁸ Recently it has also been shown that some GPCRs signal to cAMP after internalization, a G protein-dependent cascade that is generally assumed to be activated exclusively at the cell surface.⁴⁹ Cells expressing the phosphorylation deficient receptor mutant have altered expression of cell-type-specific genes, like the prestalk-specific *ecmA*,²⁹ and it will be very interesting to study how this relates to cAR1 internalization and signaling.

Improving the definition of membrane *versus* cytosol localization will help refine the present description of receptor trafficking and the use advanced single-molecule imaging with multi-color tagging of proteins and ligands will enable us to tackle these questions in detail. Conversely, fluorescence signals might be affected by other phenomena such as receptor oligomerization or endocytic acidic pH, leading to possible quenching for instance. Future work should address to what extent this can modulate the overall measures.

Conclusion

The sensitivity of single-molecule microscopy allowed for the quantitative detection of internalization of the G-protein coupled receptor, cAR1, in live *D. discoideum* cells. Our data suggest that phosphorylation-dependent cAR1 internalization is a component of the cell physiological response during development and necessary for proper progress through the developmental cycle. Probably the phosphorylation dependent internalization is induced to manage the high sustained levels of cAMP in the mound stage and these intrinsically internalized receptors are able to participate in the intracellular signaling and transcriptional regulation required for completing the developmental program.

The results showed that our methodology can be viewed as a universal tool for various types of GPCRs in all cell types. Given the involvement of GPCRs in fundamental biological processes, GPCRs by far represent the largest class of targets for modern drugs. Considering that a GPCR needs to be accessible to the drug, knowledge on GPCR internalization resulting from this methodology will minimize effective drug concentration in therapies.

Materials and methods

cAR1-eYFP fusion protein

pYU21 plasmid (constructed by Yu Long, Peter Devreotes laboratory), a plasmid of 14.10 Kb, contains eYFP fused to the C-terminus of cAR1. This plasmid was expressed in *car1*⁻ cells by electroporation. Clones were grown up in a Petri dish in HL5 medium containing 10 $\mu\text{g ml}^{-1}$ G418. For expression of phosphorylation-deficient cAR1 tagged with eYFP (cm1234-eYFP) the C-terminal cytoplasmic domain of the site-directed mutant cm1234 (described in ref. 34) was amplified by PCR using primers CACCTATTTGAGTGTATCCC and GGCTAGCTGGTGGATTATTCCTTGACCATTG and subcloned in place of the corresponding wild-type sequence in pYU21 by replacement of a BstXI-NheI fragment. Cell-lines were maintained in 6-well plates in axenic medium with addition of penicillin and streptomycin at 22 °C. Cells were maintained overnight in low fluorescence medium⁵⁰ and starved for 4–6 h in phosphate buffer prior to single-molecule measurement. All measurements were performed at 22 °C or 10 °C to slow down dephosphorylation kinetics.

Immunoblotting

cAR1-eYFP/*car1*⁻ cells were developed in 10 mM phosphate buffer (PB), pH 6.5, at a density of 10⁷ cells ml⁻¹ for 6 h.

First, cells were pre-incubated with 5 mM caffeine for 30 min and stimulated for different time periods with 10 μ M cAMP and 10 mM DTT. After centrifugation at 1500 g for 2 min cells were re-suspended to 2×10^8 cells ml⁻¹ in cold PB supplemented with a protease inhibitor cocktail (Complete™ Mini EDTA-free, Roche). The cells were lysed through a nuclear pore filter with a pore size of 3 μ m. This pore size separates the plasma membrane from cytosolic compartment-membranes.³⁷ The lysate was centrifuged at 10 000 g for 2 min. A sample of the supernatant was mixed with SDS-buffer to a density of 10^8 cells equivalent/ml. The pellet was washed with PB and solubilized with SDS-buffer to a density of 10^8 cells equivalent/ml. The supernatants and membrane protein fractions were resolved by SDS-PAGE on 10% gels along with a set of protein MW standards. cAR1-eYFP was detected by immunoblot with anti-GFP antibody (Clontech, Palo Alto).

Cells from mound stage

Cells were allowed to aggregate under PB and the resulting mounds that come off the glass were sucked into a pipet. The cells in the mounds were disaggregated by vigorous pipetting and plated on glass after which they were measured immediately.

Single-molecule microscopy

The experimental set-up for single molecule imaging has been described in detail previously.⁵¹ The optimization of single molecule imaging for *Dictyostelium* has been described in.^{30,32} The samples were mounted onto an inverted microscope (Zeiss) equipped with a 100x objective (NA = 1.4, Zeiss). A region-of-interest was set to 50 \times 50 pixel at a pixel-size of 220 nm. Measurements were done by illumination of the samples for 3 ms at 514 nm (Ar⁺-laser, Spectra Physics) at intensity of 1 kW cm⁻². The cells were photo-bleached for a period of 2.5–5 s at an intensity of 1 kW cm⁻² prior to measurement. Use of appropriate filter combinations (DCLP 530, HQ570/80, Chroma Technology and OG 530, Schott) permitted the detection of the fluorescence signal by a liquid nitrogen-cooled CCD-camera (Princeton Instrument). The total detection efficiency of the experimental setup is 8%. A stack of 100 images were recorded with a timelag between the images of $t_{lag} = 5$ ms. Images were analyzed using programs written in Matlab.³⁰

Individual receptors were identified as described previously.³² In short, a sliding mean image from the image stack was generated with Gaussian weight around the current image and subsequently subtracted from the current image in the image stack. The background-subtracted image was filtered using a Gaussian correlation filter and a threshold criterion, which was determined from the image noise, yielded starting values for a non-linear fitting procedure of two dimensional Gaussian profiles to the original images. The fitting results yielded the position, signal and background of an individual fluorescence peak. The position of a molecule was determined with an accuracy of 40 nm and its fluorescence intensity with an uncertainty of <20%. In order to determine whether the resulting fluorescent peaks were membrane-bound or cytosolic, a plasma membrane and cytosolic compartment was generated. The plasma membrane was detected by thresholding the mean

image of the stack at its mean value above background level. This provided an automatic, reliable and reproducible detection of cell edges and the thickness of the membrane was set to 3 pixels (660 nm). The area inside the plasma membrane compartment was taken as cytosolic compartment. The membrane vs. the cytosolic fraction was now easily determined by counting the fluorescent signals in the median plane.

For extrapolation of those results to the whole cell the median fraction has to be multiplied by 3/2. Assuming that receptor localization is not polarized but homogeneous over the whole cell (as reported before),^{19,20} the ratio of receptors located at the membrane in the median plane is proportional to the total ratio for the whole cell. If we assume a spherical shape for the cell, with radius r , the volume is $4/3 \pi r^3$, and the surface is $4 \pi r^2$. Thus, the ratio of membrane to volume is $3/r$. In the median plane, which we assume as a cylinder, of height $h \sim 1 \mu$ m corresponding to the depth of focus, the volume is $\pi r^2 h$ and the surface $2 \pi r h$, leading to a ratio membrane to volume of $2/r$. Therefore, the results found in the median plane as plotted in Fig. 2 and 3 under-represent plasma membrane-localized receptors and must be corrected by a factor of 3/2.

Acknowledgements

We thank P. N. Devreotes and Minghang Zhang for providing us with cAR1-YFP and cm1234-YFP constructs, respectively. This work was supported by the Marie-Curie fellowship (to A.S.), Netherlands Organisation for Scientific Research, Chemical Sciences (to S.K) and by grant 0265158Y from the American Heart Association, Texas Affiliate (to D.H.).

References

- 1 M. I. Simon, M. P. Strathmann and N. Gautam, *Science*, 1991, **252**, 802.
- 2 D. E. Clapham, *Cell*, 1993, **75**, 1237.
- 3 E. J. Neer, *Cell*, 1995, **80**, 249.
- 4 S. S. G. Ferguson, *Pharmacol. Rev.*, 2001, **53**, 1.
- 5 K. L. Pierce, R. T. Premont and R. J. Lefkowitz, *Nat. Rev. Mol. Cell Biol.*, 2002, **3**, 639.
- 6 C. A. Parent and P. N. Devreotes, *Annu. Rev. Biochem.*, 1996, **65**, 411.
- 7 P. M. Janssens and P. J. Van Haastert, *Microbiol. Rev.*, 1987, **51**, 396.
- 8 T. J. Sun and P. N. Devreotes, *Genes Dev.*, 1991, **5**, 572.
- 9 R. L. Johnson, C. L. Saxe III, R. Gollop, A. R. Kimmel and P. N. Devreotes, *Genes Dev.*, 1993, **7**, 273.
- 10 C. L. Saxe III, G. T. Ginsburg, J. M. Louis, R. Johnson, P. N. Devreotes and A. R. Kimmel, *Genes Dev.*, 1993, **7**, 262.
- 11 J. M. Louis, G. T. Ginsburg and A. R. Kimmel, *Genes Dev.*, 1994, **8**, 2086.
- 12 W. Roos, V. Nanjundiah, D. Malchow and G. Gerisch, *FEBS Lett.*, 1975, **53**, 139.
- 13 T. J. Sun, P. J. Van Haastert and P. N. Devreotes, *J. Cell Biol.*, 1990, **110**, 1549.
- 14 P. J. Van Haastert, *J. Cell Biol.*, 1983, **96**, 1559.
- 15 C. A. Parent and P. N. Devreotes, *Science*, 1999, **284**, 765.
- 16 J. Brzostowski, C. Johnson and A. Kimmel, *Curr. Biol.*, 2002, **12**, 1199.
- 17 K. Abe and K. Yanagisawa, *Dev. Biol.*, 1983, **95**, 200.
- 18 J. Y. Kim, J. A. Borleis and P. N. Devreotes, *Dev. Biol.*, 1998, **197**, 117.
- 19 M. Wang, P. J. Van Haastert, P. N. Devreotes and P. Schaap, *Dev. Biol.*, 1988, **128**, 72.

- 20 Z. Xiao, N. Zhang, D. B. Murphy and P. N. Devreotes, *J. Cell Biol.*, 1997, **139**, 365.
- 21 S. S. Ferguson, *Pharmacol. Rev.*, 2001, **53**, 1.
- 22 R. J. Lefkowitz, *Trends Pharmacol. Sci.*, 2004, **25**, 413.
- 23 M. J. Caterina, P. N. Devreotes, J. Borleis and D. Hereld, *J. Biol. Chem.*, 1995, **270**, 8667.
- 24 M. J. Caterina, D. Hereld and P. N. Devreotes, *J. Biol. Chem.*, 1995, **270**, 4418.
- 25 R. A. Vaughan and P. N. Devreotes, *J. Biol. Chem.*, 1988, **263**, 14538.
- 26 J. Y. Kim, R. D. Soede, P. Schaap, R. Valkema, J. A. Borleis, P. J. Van Haastert, P. N. Devreotes and D. Hereld, *J. Biol. Chem.*, 1997, **272**, 27313.
- 27 W. F. Loomis, *Microbiol. Rev.*, 1996, **60**, 135.
- 28 J. Williams, *Curr. Opin. Genet. Dev.*, 1995, **5**, 426.
- 29 C. Briscoe, J. Moniakis, J. Y. Kim, J. M. Brown, D. Hereld, P. N. Devreotes and R. A. Firtel, *Dev. Biol.*, 2001, **233**, 225.
- 30 S. de Keijzer, A. Serge, F. van Hemert, P. H. M. Lommerse, G. E. M. Lamers, H. P. Spaink, T. Schmidt and B. E. Snaar-Jagalska, *J. Cell Sci.*, 2008, **121**, 1750.
- 31 T. Schmidt, G. J. Schutz, W. Baumgartner, H. J. Gruber and H. Schindler, *Proc. Natl. Acad. Sci. U. S. A.*, 1996, **93**, 2926.
- 32 S. De Keijzer, B. E. Snaar-Jagalska, H. P. Spaink and T. Schmidt, in *Single Molecules and Nanotechnology*, Springer, 2008, vol. 12, pp. 107–129.
- 33 G. S. Harms, L. Cognet, P. H. Lommerse, G. A. Blab and T. Schmidt, *Biophys. J.*, 2001, **80**, 2396.
- 34 D. Hereld, R. Vaughan, J. Y. Kim, J. Borleis and P. Devreotes, *J. Biol. Chem.*, 1994, **269**, 7036.
- 35 P. J. Van Haastert, *J. Biol. Chem.*, 1987, **262**, 7705.
- 36 P. J. Van Haastert, R. Van Driel, B. Jastorff, J. Baraniak, W. J. Stec and R. J. De Wit, *J. Biol. Chem.*, 1984, **259**, 10020.
- 37 B. E. Snaar-Jagalska and P. J. Van Haastert, *Methods Enzymol.*, 1994, **237**, 387.
- 38 P. Gaudet, J. G. Williams, P. Fey and R. L. Chisholm, *BMC Genomics*, 2008, **9**, 130.
- 39 H. Padh and S. Tanjore, *FEBS Lett.*, 1995, **368**, 358.
- 40 P. J. Van Haastert, M. Wang, A. A. Bominaar, P. N. Devreotes and P. Schaap, *Mol. Biol. Cell*, 1992, **3**, 603.
- 41 M. J. Lohse, *Biochim. Biophys. Acta, Mol. Cell Res.*, 1993, **1179**, 171.
- 42 P. Tsao, T. Cao and M. von Zastrow, *Trends Pharmacol. Sci.*, 2001, **22**, 91.
- 43 M. Iijima and P. Devreotes, *Cell*, 2002, **109**, 599.
- 44 F. I. Comer and C. A. Parent, *Cell*, 2002, **109**, 541.
- 45 G. R. Schnitzler, C. Briscoe, J. M. Brown and R. A. Firtel, *Cell*, 1995, **81**, 737.
- 46 T. Araki, M. Gamper, A. Early, M. Fukuzawa, T. Abe, T. Kawata, E. Kim, R. A. Firtel and J. G. Williams, *EMBO J.*, 1998, **17**, 4018.
- 47 S. Mohanty, K. A. Jermyn, A. Early, T. Kawata, L. Aubry, A. Ceccarelli, P. Schaap, J. G. Williams and R. A. Firtel, *Development*, 1999, **126**, 3391.
- 48 M. von Zastrow, *Biochem. Soc. Trans.*, 2001, **29**, 500.
- 49 D. Calebiro, V. O. Nikolaev and M. J. Lohse, *J. Mol. Endocrinol.*, 2010, **45**, 1.
- 50 T. Liu, C. Mirschberger, L. Chooback, Q. Arana, Z. Dal Sacco, H. MacWilliams and M. Clarke, *J. Cell Sci.*, 2002, **115**, 1907.
- 51 G. S. Harms, L. Cognet, P. H. Lommerse, G. A. Blab, H. Kahr, R. Gamsjager, H. P. Spaink, N. M. Soldatov, C. Romanin and T. Schmidt, *Biophys. J.*, 2001, **81**, 2639.